

An Assessment of the GLE Alert++ Warning System

Helen Mavromichalaki ^{1,*}, Pavlos Paschalis ¹, Maria Gerontidou ¹ , Anastasia Tezari ¹, Maria-Christina Papailiou ¹, Dimitra Lingri ¹, Maria Livada ¹, Argyris Stassinakis ¹ , Norma Crosby ² and Mark Dierckxsens ²

¹ Athens Cosmic Ray Group, Faculty of Physics, National and Kapodistrian University of Athens, 15784 Athens, Greece; ppaschalis@phys.uoa.gr (P.P.); mgeront@phys.uoa.gr (M.G.); anatez@med.uoa.gr (A.T.); mpapahl@phys.uoa.gr (M.-C.P.); dlingri@phys.uoa.gr (D.L.); mairiliv@phys.uoa.gr (M.L.); a-stassinakis@phys.uoa.gr (A.S.)

² Royal Belgian Institute for Space Aeronomy, 1180 Brussels, Belgium; norma.crosby@aeronomie.be (N.C.); mark.dierckxsens@aeronomie.be (M.D.)

* Correspondence: emavromi@phys.uoa.gr; Tel.: +30-(210)-727-6890

Abstract: Over the last years the Athens Cosmic Ray Group of the National & Kapodistrian University of Athens has implemented a warning tool called GLE Alert, which is a highly credible application that issues alerts when a ground level enhancement (GLE) starts due to very high energy solar energetic particles reaching the Earth. This application warns of a high intensity solar energetic particle event up to several minutes before it reaches near the near-Earth space environment. In this work, an assessment of the latest updated version of GLE Alert, GLE Alert++, is presented. GLE Alert++ is a federated product of the ESA S2P SWE Space Radiation Expert Service Centre, which is part of the ESA Space WEather Service NETwork (SWESNET) project. The assessment of the GLE Alert++, which was finalized in October 2022, focused on: (a) the availability of the real-time data provided by the neutron monitor stations that contribute to the GLE Alert++, (b) the behaviour of each station regarding the different Alert levels status (Watch, Warning and Alert), and (c) the definition of the real-time assessment index. The results of this work are of essential importance since they ensure a reliable and trustworthy warning tool, and can be highly useful in protecting humans during extreme solar energetic events.

Keywords: ground level enhancements; cosmic rays; neutron monitors; GLE Alert++



Citation: Mavromichalaki, H.; Paschalis, P.; Gerontidou, M.; Tezari, A.; Papailiou, M.-C.; Lingri, D.; Livada, M.; Stassinakis, A.; Crosby, N.; Dierckxsens, M. An Assessment of the GLE Alert++ Warning System. *Atmosphere* **2024**, *15*, 345. <https://doi.org/10.3390/atmos15030345>

Academic Editor: Sergey Pulinet

Received: 25 January 2024

Revised: 8 March 2024

Accepted: 10 March 2024

Published: 12 March 2024



Copyright: © 2024 by the authors. Licensee MDPI, Basel, Switzerland. This article is an open access article distributed under the terms and conditions of the Creative Commons Attribution (CC BY) license (<https://creativecommons.org/licenses/by/4.0/>).

1. Introduction

The ground level enhancements (GLEs) of the cosmic ray intensity (CRI), as well as the physical process leading to their occurrence, are well known phenomena that have been extensively documented in the scientific literature [1–4]. GLEs are events of a sudden increase in the CRI, with protons energies above 433 MeV [5], due to solar phenomena, such as solar flares and coronal mass ejections. The increase in the cosmic ray flux is recorded by satellites as extreme solar energetic particle events [6], in addition to ground-based detectors, such as neutron monitors (NMs) and muon detectors. For example, one astrophysical instrument that provides information on the radiation environment near the Earth is the anticoincidence shield of the spectrometer on the INTEGRAL satellite (ACS SPI). The ACS SPI detector records hard X-ray radiation with energy > 100 KeV and protons with energy > 100 MeV. The ACS SPI data are available online with a time resolution of 50 ms (<https://isdc.unige.ch/~savchenk/spiaccs-online/spiaccspnlc.pl>; accessed on 8 March 2024).

Ground-based detectors record only high-energy SEPs (>433 MeV as mentioned above), as their increased penetration power allows them to reach the detector and trigger a GLE event. On the other hand, low-energy SEPs may not penetrate the Earth's magnetic field sufficiently to be detected by the detector. The occurrence of a GLE following a SEP event is therefore related to energy levels rather than fluxes (i.e., such occurrences are

influenced by the proton's energy). In these senses, it is beyond the aim of the GLE Alert++ system to issue notification for SEPs events such as, for example, the events that occurred on 25 February 2023 and 17 July 2023, which is described in [7]. These SEP events are not identified as sub-GLEs. On the other hand, since sub-GLEs are weaker GLE events [8], they have the potential to be detected by the GLE Alert++ system.

In order to generate a GLE, the solar energetic ions must have sufficient energy to penetrate the Earth's magnetic field and then interact in the atmosphere. In this way, nuclear interactions are generated, leading to a cascade of secondary particles. Hence, a measurable increase in the total observed CRI at ground level is produced. The geomagnetic field shields the Earth from the lower energy particles. The amount of shielding is a function of geomagnetic latitude (i.e. minimum (zero) shielding is observed in the Earth's Polar Regions and maximum shielding is observed in the equatorial regions). So protons with energies greater than approximately 450 MeV can generate a nuclear cascade that can penetrate to the Earth's surface in the polar Regions. It takes approximately 15 GeV of energy to penetrate through the Earth's magnetosphere in the equatorial regions and then generate the nuclear cascades in the atmosphere. Such an increase above the cosmic radiation background intensity can be detected by cosmic ray instrumentation. The acceleration process of protons to GeV energies appears to be associated with the rapid release of energy in the solar magnetic fields, resulting in shocks in the solar corona and interplanetary space. Ground level events can be associated with a significant solar flare on the visible disk or a presumed flare from an active region that may not be on the visible solar disk. During the 23rd solar cycle, all of the GLEs were also associated with fast coronal mass ejections [9–11].

These events are rare, and only 73 events have been registered since 1942 [12,13]; however, their impact on space weather research and applications are of significant importance, since they can affect sensitive technological systems and human health. It is now well recognized that solar proton events can adversely affect space and ground-based systems. The high energy solar proton events known as GLEs have a harder spectrum and deposit increased radiation in polar and mid latitude regions. The higher energy particles also significantly impact solar cells and star sensor pointing systems on spacecraft, in addition to producing an overall increase in the impact of the radiation environment on spacecraft components and transpolar aircraft flights. So, a GLE alert system provides crucial information for a wide range of space and ground-based systems. SEPs that propagate to Earth can cause damage to satellite electronics and can pose a radiation hazard to astronauts and air crews. In a typical SEP event, the particle flux increases in the 10–100 MeV energy range, but these energies are insufficient to produce an effect on ground level detectors. However, in the most extreme SEP events, the particle flux at energies >500 MeV is also increased, but this increase can be detected by ground-based neutron monitors as a GLE. In addition, because the propagation speed of SEPs along the interplanetary magnetic field depends upon energy, the start time of the intensity increase in the neutron monitors is earlier than that of the low-energy proton flux. Furthermore, when energy is higher, less time is required to reach maximum intensity. Consequently, GLE observations make it possible to issue earlier warnings of the arrival of the SEP event than methods based upon charged particles with lower energy. For this reason, it is necessary to have forewarning systems that can provide accurate and timely GLE alerts.

Important attempts with this purpose have been undertaken over the years, with the three most recognized and accurate being the alert system by Bartol University [14], the alert system by the IZMIRAN group [15], and the GLE Alert systems by the Athens Cosmic Ray Group and the Athens Neutron Monitor Station (A.Ne.Mo.S.) [16–18].

In this study, an assessment of the latest version of the GLE Alert system, "GLE Alert++" is presented. A brief description of GLE Alert++ and the operation method is provided. Moreover, the availability of the real-time data provided by NMs that contribute to GLE Alert, the behaviour of each station regarding the different alert levels statuses (watch, warning and alert), and the definition of the real-time assessment index are analysed. Finally, the results are discussed and conclusions are given.

2. GLE Alert++

The GLE Alert service has been operating at the Athens Neutron Monitor Station (A.Ne.Mo.S) since 2009. The service started as GLE Alert, was upgraded to GLE Alert Plus and currently operates as GLE Alert++. GLE Alert++ is available on the ESA SWE portal as a federated product under the “Space Radiation Expert Service Centre”, as part of the ESA Space WEather Service NETwork (SWESNET) project (<https://swe.ssa.esa.int/anemos-federated>; accessed on 8 March 2024).

As the previous software, the GLE Alert++ requires of selected NMs to provide 1 min resolution data, updated every 1 min. An automated real-time GLE Alert is the output of the application. The real-time GLE Alert++ status is implemented and provided to ESA SSA SWE R-ESC using a graphical web interface. Although the main core of the GLE Alert++ software remains the same as the previous system, there are important upgrades of its software design, web page information, and functionality. More details about this version of the application and its improvements on the oldest one are presented in [18].

It is important to note that there are four different levels in the GLE Alert system. Watch status refers to a case in which three consequent measurements from one NM exceed its own threshold value, with the result that this NM entered into station alert mode. Warning status refers to a case when two NM stations were in alert mode. General Alert is issued when three stations’ alert points are marked in succession within a time window of 15 min. When there is no station alert mode, the general status is quiet.

Since the GLE Alert service has been in operation, it has provided valid alerts, operated in a highly reliable manner with minimum missed events, and issued alerts of several minutes, enabling the scientific community to take all necessary actions to protect both humans and technological systems. The most recent example is the alert for GLE 73, on 28 October 2021 at 16:06 UT based on the neutron monitor stations at Fort Smith (FSMT) (Canada), South Pole Bares (SOPB) (Antarctica) and South Pole (SOPO) (Antarctica) [18].

The service is based on an algorithm that uses NM data downloaded from the high-resolution neutron monitor database (NMDB) every minute, or as soon as the stations send their measurements (www.nmdb.eu; accessed on 8 March 2024) [16,19]. While data in the NMDB database exists in three formats (uncorrected data, corrected for pressure, corrected for pressure and efficiency), the algorithm only uses the ‘corrected for efficiency’ data.

It should be emphasized that the accurate operation of this service is based on two parameters, namely the real time behavior of NM stations and the quality of their data. If an abrupt increase in the CRI is recorded simultaneously by three stations, an alert is raised. This increase of the CRI is calculated by comparing the current cosmic ray flux with a baseline formed by the average of the cosmic ray flux during the last 60 min. When a measurement is over a specific trust interval, then the station enters watch mode. If the measurement of the following minute remains over this trust interval, the station enters warning mode. Finally, if the following value remains over the trust interval, then the station enters alert mode. From the moment the station enters alert mode, it remains in this mode for 15 min. If three stations are simultaneously in alert mode, then the service raises a general alert. The functionality and algorithm of GLE alert systems are analytically described in [17,18].

Data

In order to take into account the most recent status of NM stations, this study covered the time period from 1 January 2020 until 31 August 2022. This is a relatively long period, which allows us to determine the behaviour of the NM stations.

The GLE Alert++ service needs timely and reliable real-time data. Data from thirty-four (34) NM stations feed into the GLE Alert++ algorithm. The stations, along with their characteristics (geographic coordinates, altitude, cut-off rigidity, fraction of 1-min data records) are presented in Table 1. The eight stations that were not active during the assessment period are indicated with a grey background, including the three stations (BURE, ESOI, MCMU) that were closed and the stations (MCRL, MGDN, MOSC, MRNY,

NVBK) that had a temporary network connection problem during the examined period (the last five stations may become available in the future).

Table 1. List of NM stations with characteristics being used in the current version of GLE Alert++. Stations not active during the assessment period have a grey background.

No	NM Station	Abbr.	Geogr. Coordinates	Altitude (m)	Cut-Off Rigidity (GV)	Downtime Fraction (%)
1	Alma Ata, Kazakhstan	AATB	43.14° N 76.60° E	3340	6.69	9%
2	Apatity, Russia	APTY	67.57° N 33.40° E	177	0.65	0%
3	Athens, Greece	ATHN	37.97° N 23.78° E	260	8.53	3%
4	Baksan, Russia	BKSN	43.28° N 42.69° E	1700	5.60	0%
5	Plateau de Bure, France	BURE	44.38° N 5.54° E	2555	5.00	100%
6	Castilla-La Mancha, Spain	CALM	40.33° N 3.90° E	708	6.95	19%
7	Emilio Segre, Israel	ESOI	33.30° N 35.80° E	2055	10.75	100%
8	Fort Smith, Canada	FSMT	60.02° N 111.93° W	180	0.30	10%
9	Inuvik, Canada	INVK	68.36° N 133.72° W	21	0.30	1%
10	Irkutsk 2, Russia	IRK2	52.37° N 100.55° E	2000	3.64	55%
11	Irkutsk 3, Russia	IRK3	51.29° N 100.55° E	3000	3.64	46%
12	Irkutsk, Russia	IRKT	52.47° N 104.03° E	475	3.64	27%
13	Jungfrauoch, Switzerland	JUNG	46.55° N 7.98° E	3570	4.50	0%
14	Jungfrauoch 1, Switzerland	JUNG1	46.55° N 7.98° E	3475	4.50	0%
15	Kerguelen, Indian Ocean	KERG	49.35° S 70.25° E	33	1.14	3%
16	Kiel 2, Germany	KIEL2	54.34° N 10.12° E	54	2.36	0%
17	Lomnický štít, Slovakia	LMKS	49.20° N 20.22° E	2634	3.84	0%
18	Mc Murdo, Antarctica	MCMU	77.95° S 166.60° E	48	0.30	100%
19	Mobile CR Laboratory, Russia	MCRL	55.47° N 37.32° E	2000	2.43	100%
20	Magadan, Russia	MGDN	60.04° N 151.05° E	220	2.10	100%
21	Moscow, Russia	MOSC	55.47° N 37.32° E	200	2.43	100%
22	Mirny, Antarctica	MRNY	66.55° N 93.02° E	30	0.03	100%
23	Nain, Canada	NAIN	56.55° N 61.68° W	46	0.30	16%
24	Newark, USA	NEWK	39.68° N 75.75° W	50	2.40	10%
25	Novosibirsk, Russia	NVBK	54.48° N 83.00° E	163	2.91	100%
26	Oulu, Finland	OULU	65.05° N 25.47° E	15	0.81	0%
27	Peawanuk, Canada	PWNK	54.98° N 85.44° W	53	0.30	24%
28	Rome, Italy	ROME	41.86° N 12.47° E	0	6.27	1%
29	South Pole Bare, Antarctica	SOPB	90.00° S N/A	2820	0.10	5%
30	South Pole, Antarctica	SOPO	90.00° S N/A	2820	0.10	5%
31	Terre Adelie, Antarctica	TERA	66.65° S 140.00° E	32	0.00	6%
32	Thule, Greenland	THUL	76.50° N 68.70° W	26	0.30	3%
33	Tixie Bay, Russia	TXBY	71.01° N 128.54° E	0	0.48	0%
34	Yakutsk, Russia	YKTK	62.01° N 129.43° E	105	1.65	0%

In order to determine the stations that would be included in the assessment, and consequently be used in the updated GLE Alert product, this study was expanded to include all existing NM stations beyond the aforementioned 34 stations. The NMDB provides data from seventy-one (71) NM stations. The main characteristics (geographic coordinates, altitude, cut-off rigidity, fraction of 1-min data records) from 1 January 2020 to 31 August 2022 (1,401,120 min) of the additional thirty-seven (37) stations are presented in Table 2.

In Table 2 it can be seen that twenty-two (22) of the thirty-seven (37) remaining NM stations that are currently not used by GLE Alert++ are inactive, while fifteen (15) NMs are in operation and could potentially be included in the GLE Alert++ system. Specifically, the DRBS NM station (Dourbes, Belgium geographic coordinates: 50.10° N 4.60° E, altitude: 225 m, cut-off rigidity: 3.18 GV, and a number of 1-min records after 1 January 2020: 1,427,770) presents an acceptable real-time behaviour. The inactive stations are again indicated by a grey background.

Table 2. The 37 NM stations with characteristics not being used in the current version of GLE Alert++. Inactive stations have a grey background.

No	NM Station	Abbr.	Geogr. Coordinates	Altitude (m)	Cut-Off Rigidity (GV)	Downtime Fraction (%)
1	Almaty, Kazakhstan	AATA	43.25° N 76.92° E	897	5.90	42%
2	Ahmedabad, India	AHMD	23.01° N 72.61° E	50	15.94	100%
3	Aragats, Armenia	ARNM	40.22° N 44.15° E	3200	7.10	100%
4	Barentsburg, Spitzbergen	BRBG	78.06° N 14.22° E	51	0.00	3%
5	Calgary, Canada	CALG	51.08° N 24.13° W	1123	1.08	95%
6	Climax, USA	CLMX	39.37° N 106.18° W	3400	3.03	100%
7	Daejeon, South Korea	DJON	36.39° N 127.37° E	200	11.20	84%
8	Mini Dome Bare, Antarctica	DOMB	75.06° S 123.20° E	3233	0.01	32%
9	Mini Dome C, Antarctica	DOMC	75.06° S 123.20° E	3233	0.01	0%
10	Dourbes, Belgium	DRBS	50.10° N 4.60° E	225	3.18	0%
11	Dourbes2, Belgium	DRBS2	50.10° N 4.60° E	225	3.18	100%
12	Durham, USA	DRHM	43.10° N 70.83° W	0	1.58	100%
13	Haleakala1, Hawaii	HLE1	20.72° N 156.28° W	3052	13.30	100%
14	Hermanus, South Africa	HRMS	34.43° S 19.23° E	26	4.58	80%
15	Huancayo, Perou	HUAN	12.03° S 75.33° W	3400	13.45	100%
16	Jang Bogo, Antarctica	JBGO	74.6° S 164.2° E	30	0.30	87%
17	Kingston, Australia	KGSN	42.99° S 147.29° E	65	1.88	100%
18	Kiel, Germany	KIEL	54.34° N 10.12° E	54	2.36	100%
19	Leadville, USA	LDVL	39.15° N 106.14° W	3094	3.03	100%
20	Mt. Wellington, Australia	MTWS	42.92° S 147.25° E	725	1.80	100%
21	Mawson, Antarctica	MWSN	67.60° S 62.88° E	0	0.22	13%
22	Mexico City, Mexico	MXCO	19.33° N 260.82° E	2274	8.20	4%
23	Nor-Amberd, Armenia	NANM	40.22° N 44.15° E	2000	7.10	53%
24	Neumayer III, Antarctica	NEU3	70.38° S 8.15° W	40	0.10	100%
25	Norilsk, Russia	NRLK	69.26° N 88.05° E	0	0.63	7%
26	Ny-Alesund, Spitzbergen	NYAA	78.90° N 11.90° E	0	0.00	100%
27	Observatorio de Rayos C3smicos Ant3rtico, Antarctica	ORCA	62.39° S 60.23° W	12		100%
28	Observatorio de Rayos C3smicos Ant3rtico B, Antarctica	ORCB	62.39° S 60.23° W	12		100%
29	Polarstern, Atlantic Ocean	POL1	Antarctica, ship	0		100%
30	Doi Inthanon, Thailand	PSNM	18.59° N 98.49° E	2565	16.80	100%
31	Potchefstroom, South Africa	PTFM	26.68° S 27.09° E	1351	6.94	58%
32	Sanae VIII, Antarctica	SANB	70.31° S 02.40° W	52	0.73	100%
33	Sanae IV, Antarctica	SNAE	71.40° S 02.51° W	856	0.73	100%
34	Tibet, China	TIBT	30.11° N 90.53° E	4300	14.10	100%
35	Tsumeb, Namibia	TSMB	19.20° S 17.58° E	1240	9.15	91%
36	Zugspitze, Germany	UFSZ	47.40° N 11.00° E	2650	4.10	100%
37	Zugspitze, Germany	ZUGS	47.42° N 10.98° E	2960	4.24	100%

3. Assessment of the GLE Alert++

The assessment of the GLE Alert ++ performance includes: (1) a study of the availability of real-time data provided by the NM stations that contribute to the GLE Alert++, (2) the behaviour of each station regarding the different levels of Alert, and (3) a real-time assessment index that refers to the real-time behaviour of each NM station, which is not only correlated with the measurement delays but also with the existence of all measurements.

It should be emphasized that in this work no conclusions were drawn about the quality of the cosmic ray data, as this of course remains the responsibility of the principal investigator of each NM station. In order to identify the stations that will be used by the GLE Alert++ service in the future, only the availability of the real-time data and the data flow of each station are assessed and discussed in the following.

3.1. Availability of Real-Time Data

The assessment of real-time data was only applied to the active stations obtained by the above-mentioned analysis. By applying an SQL query from the NMDB database, the delay between the time each measurement was registered and provided in the database was calculated. The delays of all measurements were calculated and a frequency table with 1-min bins of delay was generated for each NM station for every month.

The tables showing the number of occurrences of delay at stations used and unused by the GLE Alert++ were plotted in a three-dimensional diagram. The x-axis of the diagram is the corresponding month, the y-axis is the delay bin, and the z-axis is the number of occurrences of delay. Each delay bin indicates one minute. An example of such a plot is presented in Figure 1, both for the ATHN station used by the GLE Alert++ (a) and the NRLK station not used by the GLE Alert++ (b), respectively. It is important to note that the diagrams were only plotted for stations that presented delays of up to 20 min.

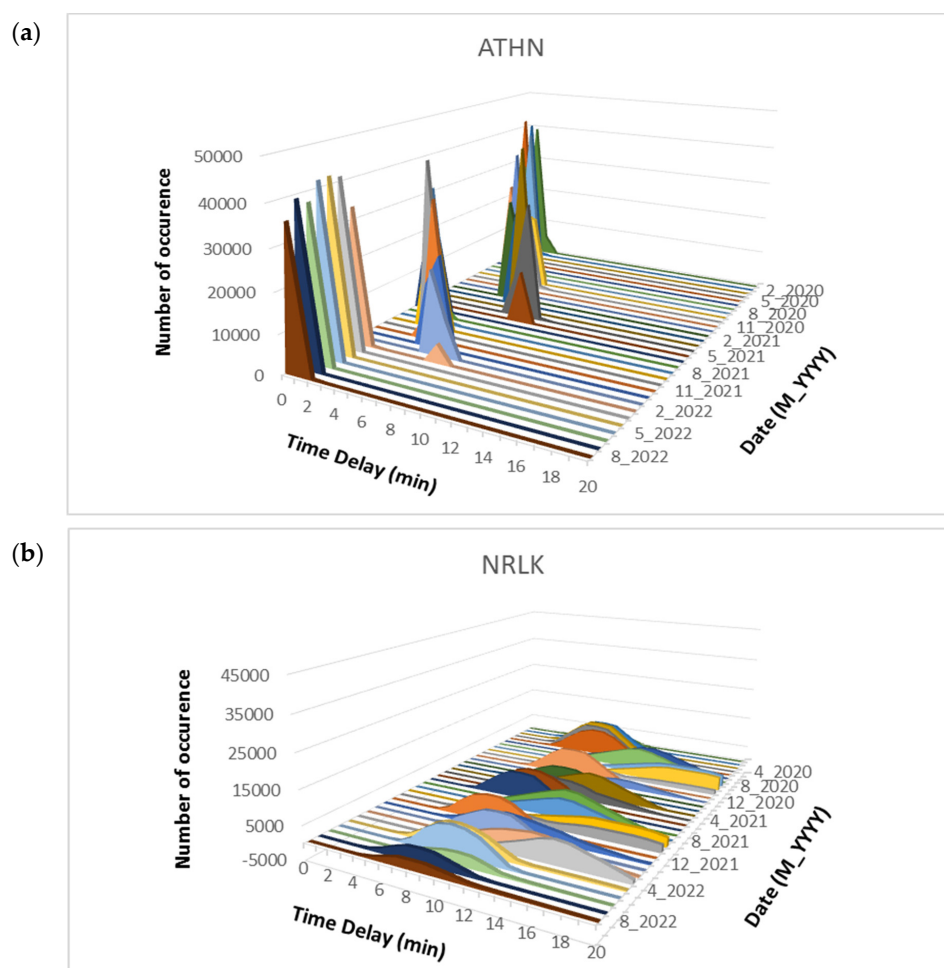


Figure 1. The occurrence of delay tables of the ATHN (a) and NRLK (b) NM station, illustrated in a three-dimensional diagram. The x-axis of the diagram is the corresponding month, the y-axis is the delay bin, and the z-axis is the number of occurrences of delay.

The smaller the delay, the better the station’s real-time behaviour. At this point, it is important to note that the real-time behaviour of some stations during the last months of 2022 appears to have improved, presenting shorter delays than in the past. This may be because the stations have upgraded their infrastructure and systems. So in this case such stations are not excluded from the analysis. The previous months are useful to determine the stability of the NM stations.

3.2. Assessment of the Different Levels of Alert Mode

The frequency occurrence of each alert level (watch, warning and alert), per each station and per each month, was calculated. According to the physical concept of the algorithm, a station enters into alert mode due to an increase of the cosmic ray flux; however, it is possible the station also does this because of system errors. The GLE Alert algorithm was applied to the historical data of the NM stations in order to count how many times a station entered warning, watch or alert mode. An example of these results is shown in Tables 3 and 4, which depict the “alert” assessment for some of the stations used in the current version of the GLE Alert++ (Table 3) and for some stations not used in the current version of the GLE Alert++ (Table 4). Similar tables were generated for the three assessment categories (watch, warning and alert) for stations listed in Tables 1 and 2 with a white background. For these three assessment categories, the following colour coding is used:

- Watch assessment (green colour corresponds to 0–1300 watch modes in each month, yellow to 1301–1360 watch modes, and red to watch modes greater than 1361).
- Warning assessment (green colour corresponds to 0–60 warning modes in each month, yellow to 61–70 warning modes, and red to warning modes greater than 71).
- Alert assessment (green colour corresponds to 0–6 alert modes in each month, yellow to 7–9 alert modes, and red to alert modes greater than 10).

The above-mentioned numbers correspond to the times a station enters watch, warning and alert mode, respectively, during the period of the study. Since the disturbed periods are a very small fraction of the whole period, a value greater than the expected statistical counterpart means the station entered disturbed mode more times than was statistically expected. As a result, its data presents abrupt increases that are not correlated to the actual increase of the CRI.

Table 3. The times a NM station enters “alert” mode. Results refer to some of the NM stations used in GLE Alert++. The colour coding is described in the text.

MM.YYYY	NMs Used in the Current Version of GLE Alert++ (from Table 1)										JUNG	JUNG1	KERG	
	AATB	APTY	ATHN	BKSN	CALM	FSMT	INVK	IRK2	IRK3	IRKT				
08.2022	1	4	1	3	4	2	2		2	2	2	2	2	4
07.2022	1	1	2	6	2	2	2		0	0	2	1	5	
06.2022	1	4	1	3	1	1	1	1	1	0	0	2	2	
05.2022	2	4	2	1	1	1	0	3	2		1	1	6	
04.2022	1	2	0	1	1	3	2	3	6	8	2	4	2	
03.2022	1	3	2	2	3	2	2	3	3	3	1	4	5	
02.2022	0	3	2	2	1	2	1	3	2	2	2	1	6	
01.2022	1	4	0	4	0	2	1	1	4	0	1	1	3	
12.2021	1	1	2	2	1	1	1	1	1	3	3	2	4	
11.2021	1	2	1	1	2	5	4	2	0	5	2	6	8	
10.2021	0	4	2	0	3	2	3				2	1	5	
09.2021	0	1	5	3	5	3	4				13	2	2	
08.2021	0	0	0	5	4	6	2				1	4	2	
07.2021	0	2	0	6	1	0	2				2	0	1	
06.2021	2	2	3	9	3	3	1				3	2	1	
05.2021	0	0	0	3	4	1	1			2	5	3	3	
04.2021	0	1	3	3	1	4	2			2	0	2	1	
03.2021	1	1	2	14	2	6	3			10	3	1	3	
02.2021	1	4	2	7	1	2	5		0	5	1	4	6	
01.2021	4	2	3	4	0	0	2		2	0	3	4	1	
12.2020	1	5	3	2	1	8	2		4	0	5	3	1	

Table 3. Cont.

MM.YYYY	NMs Used in the Current Version of GLE Alert++ (from Table 1)												
	AATB	APTY	ATHN	BKSN	CALM	FSMT	INVK	IRK2	IRK3	IRKT	JUNG	JUNG1	KERG
11.2020	2	2	2	4	1	7	3		4	1	1	1	2
10.2020	4	2	3	0	2	1	1		2	4	1	2	4
09.2020	1	4	1	6	0	3	0		0	0	2	2	5
08.2020	2	0	2	6	0	6	1	3	4	1	3	12	0
07.2020	1	2	1	6	2	3	0	1	2	3	0	6	2
06.2020	1	2	0	8	3	6	1	0	0	3	1	0	9
05.2020	2	2	2	5	0	10	0	3	3	2	5	5	2
04.2020	6	0	2	3		11	1	1	3	2	6	3	4
03.2020	1	6	2	3		13	0	0	10	0	3	1	2
02.2020	1	3	0	3	3	14	0	2	0	0	1	2	2
01.2020	3	2	2	6	1	11	2	2		1	3	5	3

Table 4. The times a NM station enters “alert” mode. The results refer to some NM stations not used in the GLE Alert++. The colour coding is described in the text.

MM.YYYY	NMs Not Used in the Current Version of GLE Alert++ (from Table 2)												
	AATA	BRBG	CALG	DJON	DOMB	DOMC	DRBS	HRMS	JBGO	MWSN	MXCO	NANM	NRLK
08.2022	9		0		4	0	2			3	1		0
07.2022	35	4			6	2	0			3	3		2
06.2022	55	1			11	0	9			6	4		2
05.2022		3			11	4	2			22	0		4
04.2022		1			11	1	1			2	2		1
03.2022		2			5	2	4			2	2		2
02.2022		3			3	2	3			1	2		2
01.2022		1			4	0	4			7	3		0
12.2021		2		0	3	3	3		0	1	2		2
11.2021	7	1		2	1	4	4		0	5	0		5
10.2021		0		0	0	1	1		0	62	4		0
09.2021	3	3		0	4	1	2		0	38	2		1
08.2021	3	3		5	0	2	5		0	0	2		1
07.2021	6	4		0	1	2	3		0	1	1		0
06.2021	11	5			1	0	2		0	5	1		3
05.2021	19	2			0	3	1		0	4	1	47	1
04.2021	4	0		0	1	3	3		0	37	2	8	7
03.2021	5	1			1	2	1		0	1	0	5	1
02.2021	1	1			5	1	2	0	0	6	1	1	1
01.2021	0	1			2	3	3		0	3	2	2	6
12.2020	11	4			0	4	3		0	9	4	2	4
11.2020	0	1				4	4			14	2	7	2
10.2020	10	1				0	2			4	1	2	0
09.2020	1	4				2	4			14	4	4	2
08.2020	5	3				2	5			6		12	1
07.2020	2	4				4	2	5	6	2	2	14	3
06.2020	2	1				144	8	1	4	0	1	4	3
05.2020	0	5				4	3	1		4	4	2	4
04.2020	6	1				3	1	1		1	3	2	5
03.2020	5	3				2	1	2		3	4	0	11
02.2020	6	1		0		2	2	0		3	0	1	4
01.2020	15	2		0		3	2	1		1	0	0	4

The distributions of the occurrences for the uncoloured stations in Tables 1 and 2 are given in Figure 2. It can be seen that, in every month, a station enters “watch” status about 1200–1280 times, “warning” status about 50–60 times, and “alert” status about 3–6 times. Monthly results were also calculated for each station.

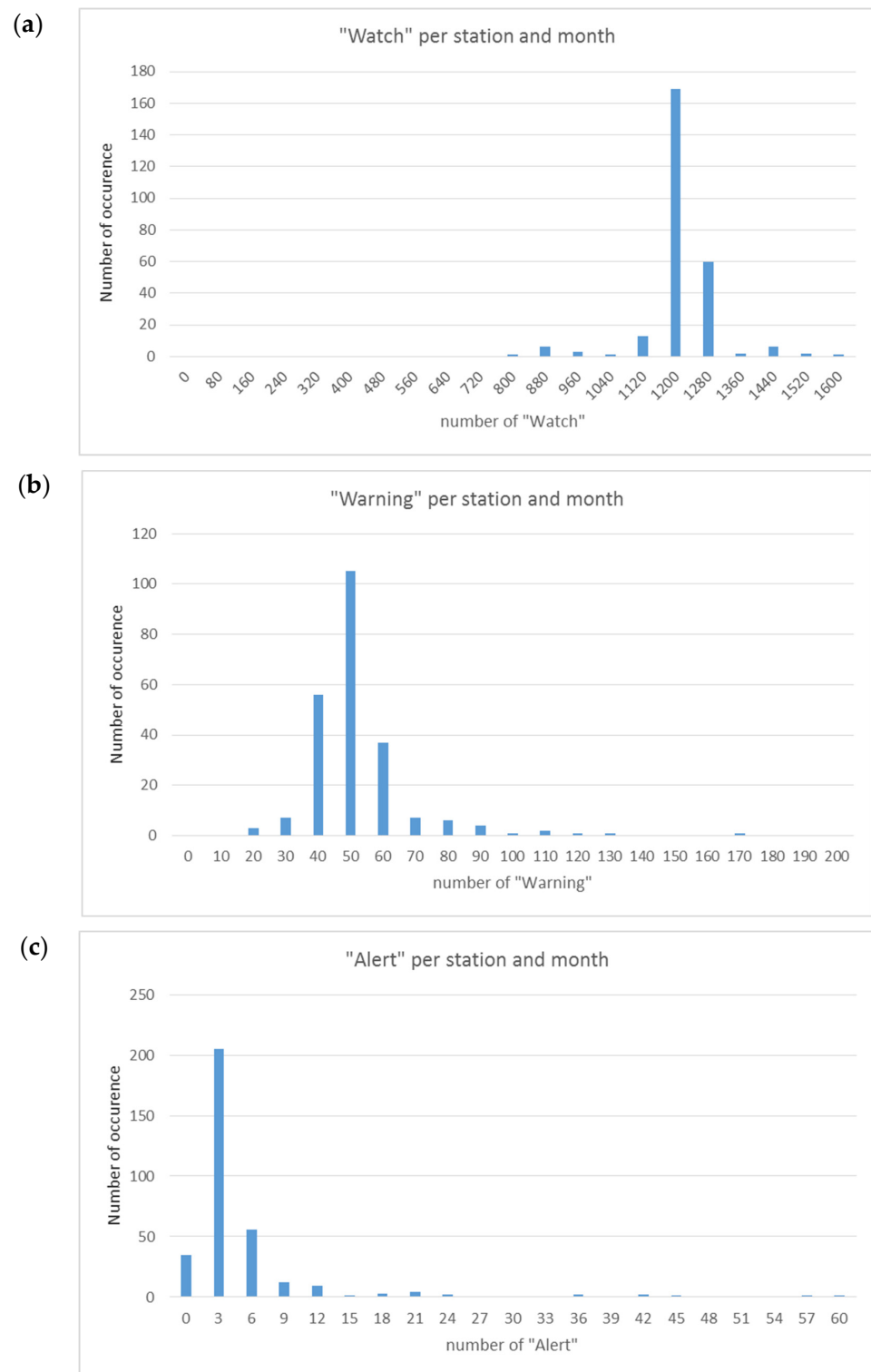


Figure 2. Distribution of occurrences for “watch” (a), “warning” (b) and “alert” (c), per station and month.

3.3. Real Time Assessment Index

The delay plots provide a visual result that in some cases is enough to identify the real-time behaviour. However, the plots themselves are not enough to assort the stations with similar visual behaviours. Moreover, the real-time behaviour is not only correlated with the measurement of delays but also with the availability of all measurements (integral

of the frequency), which is not visible in the plots. To enable further investigation, the following real-time index ('Real-time Index based on Credit Points') is defined.

According to the query, the delays are categorized in 60 bins ranging from 1 min delay to 60 min delay, plus one more bin that collects all the remaining delays of more than 60 min. The one-min delay is the minimum that can be observed because the timestamp of a NM measurement indicates the start of the measurement, and the measurement is thus sent to the database the following minute. The index is defined as follows:

$$\begin{aligned} \text{Real-time Index} = & 100 \times [61 \times \text{number of values with 1 min delay} \\ & +60 \times \text{number of values with 2 min delay} \\ & +59 \times \text{number of values with 3 min delay} \\ & + \dots \\ & +2 \times \text{number of values with 60 min delay} \\ & +1 \times \text{number of values with 61 min delay}] / 61 \times \text{total minutes of the month} \end{aligned}$$

The division with 61 × total minutes of the month corresponds to the ideal behaviour of the stations, which is a continuous operation with a one minute delay.

The index can take values from 0 to 100. If all the measurements are available during a month and all these measurements have a delay greater than 1 h, the index will be 100/61 = 1.64. However, the index can take values less than this, in instances where some measurements are not available. In a case where all measurements are absent, the index will be equal to zero. The defined index is correlated with an equivalent mean delay of the measurements. If all the measurements have 1 min delay, then the Index is 100 × 61/61 = 100. If all the measurements have 5 min delay, then the Index is 100 × 57/61 = 93.44. According to the definition, as determined in Equation (1), the equivalence between the mean delay and the index is given in Table 5.

$$\text{Equivalent Mean Delay} = 61 \times (1 - \text{Index}/100) + 1 \tag{1}$$

Table 5. The equivalent mean delay and the corresponding real-time assessment index.

Equivalent Mean Delay (min)	Real-Time Index	Equivalent Mean Delay (min)	Real-Time Index
1	100.00	16	75.41
2	98.36	17	73.77
3	96.72	18	72.13
4	95.08	19	70.49
5	93.44	20	68.85
6	91.80	21	67.21
7	90.16	22	65.57
8	88.52	23	63.93
9	86.89	24	62.30
10	85.25	25	60.66
11	83.61	26	59.02
12	81.97	27	57.38
13	80.33	28	55.74
14	78.69	29	54.10
15	77.05	30	52.46

The equivalent mean delay is necessary to correlate the real-time index to time, which is a physical quantity. It should be mentioned that the notification of an alert is useful when this takes place at the earliest time possible—in most cases, it is desirable to raise an alert within 15 min.

The distribution of the calculated values of the real time index, for all NM stations every month, is given in Figure 3. The peak at 0 value corresponds to cases when no recordings have been sent to NMDB. An example of the index results is given in Table 6 for the stations used in the current version of the GLE Alert++, and in Table 7 for the stations not used in the current version of the GLE Alert++. Results were obtained for all stations listed in Tables 1 and 2 with a white background. In these tables, values less than 77.05 (15 min equivalent delay) are indicated with red colour, values between 77.05 and 85.25 (11 to 15 min delay) with yellow, values between 85.25 and 93.44 (6 to 10 min delay) with light green, and values greater than 93.44 (5 min delay) with green. An acceptable delay of the GLE Alert service is about 15 min.

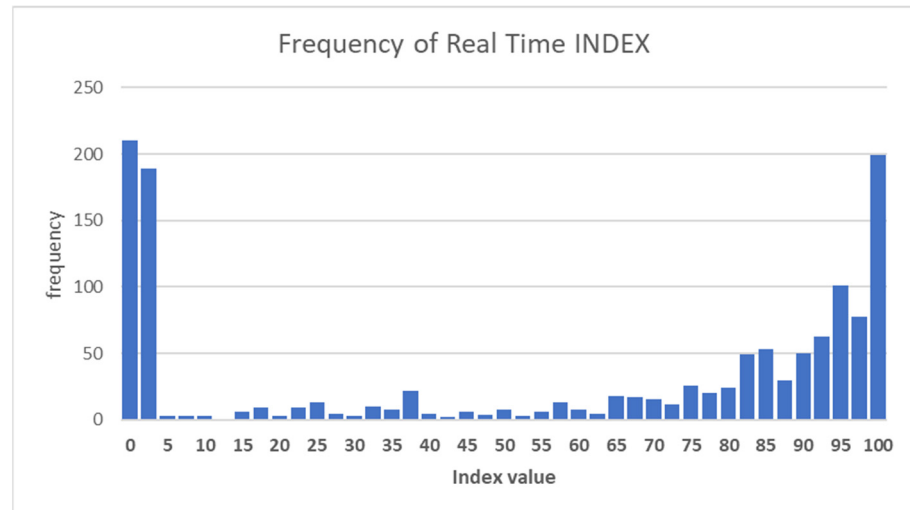


Figure 3. The frequency distribution of the real-time index values for all NM stations during the period under examination.

Table 6. Real-time index values for the NM stations used in the GLE Alert++. The colour coding is described in the text.

MM.YYYY	NMs Used in the Current Version of GLE Alert++ (from Table 1)																								
	ATB	APTY	ATHN	BKSN	CALM	FSMT	INVK	IRK2	IRK3	IRKT	JUNG	JUNG1	KERG	KIEL2	NAIN	NEWK	OULU	PWNK	ROME	SOPB	SOPO	TERA	THUL	TXBY	YKTK
08.2022	99.30	89.60	82.22	99.14	99.07	90.60	92.35	0.00	30.35	96.68	93.20	93.27	97.76	97.82	90.53	93.23	97.19	90.14	99.23	84.85	84.88	97.59	91.98	59.52	61.72
07.2022	99.23	48.69	90.80	98.17	99.35	81.00	88.51	0.00	13.04	63.01	92.91	92.97	96.27	69.59	76.82	88.39	97.86	86.76	89.41	77.91	77.98	97.66	83.91	76.74	77.18
06.2022	98.52	78.79	89.95	99.63	99.82	79.67	93.57	49.01	54.58	4.14	93.86	93.92	91.39	100.00	91.67	94.34	98.13	89.84	99.57	79.96	79.97	93.77	92.25	17.30	17.32
05.2022	94.49	86.74	96.43	39.04	99.82	90.64	94.34	72.12	90.58	0.00	94.15	94.23	97.38	96.30	89.92	87.35	98.35	93.75	99.19	90.42	90.43	95.51	92.85	80.94	82.61
04.2022	99.81	92.43	100.00	62.81	99.82	81.57	89.60	86.32	89.30	33.23	94.46	94.54	95.98	99.86	91.77	93.49	98.37	86.48	98.08	72.80	72.82	97.03	92.25	80.50	81.53
03.2022	99.97	74.75	95.33	99.71	99.82	92.43	94.10	86.12	3.08	94.15	94.80	94.87	95.03	99.98	91.44	87.53	98.37	92.54	98.53	86.07	83.59	98.00	92.52	79.85	81.79
02.2022	96.43	99.43	97.57	99.91	84.90	91.62	94.16	82.98	63.82	93.12	95.11	95.16	95.46	99.86	89.91	89.85	98.36	90.15	89.18	91.42	91.43	97.16	92.31	84.05	81.62
01.2022	99.79	62.59	62.89	99.69	15.09	49.50	94.09	79.01	83.51	88.42	95.23	95.28	89.16	99.84	57.47	90.40	98.06	92.61	98.95	89.85	89.91	94.53	92.59	80.53	83.25
12.2021	99.40	87.00	83.33	88.33	75.66	81.89	94.00	90.08	75.78	96.55	95.73	95.79	94.63	99.17	1.64	94.53	98.18	83.11	99.64	92.04	92.05	88.24	92.17	82.95	82.46
11.2021	98.44	69.53	89.48	97.61	98.25	72.87	92.79	45.71	0.71	16.36	94.52	94.56	75.52	98.44	31.58	92.88	96.83	92.37	97.76	90.74	90.66	90.84	88.19	81.96	82.06
10.2021	93.21	66.55	94.22	98.93	99.77	94.32	91.91	0.17	0.00	0.00	95.54	96.41	92.79	100.00	93.80	92.07	98.37	92.97	99.42	93.87	93.85	97.60	93.52	81.72	82.85
09.2021	99.99	60.71	93.51	99.82	99.79	87.58	92.84	0.14	0.00	0.00	96.66	96.72	94.05	100.00	93.68	95.66	96.40	93.40	99.32	92.16	92.30	98.05	94.51	76.78	86.06
08.2021	96.85	63.12	78.20	97.92	99.85	79.65	89.76	0.13	0.00	0.00	97.00	97.05	88.29	100.00	93.31	94.49	98.39	94.96	97.68	95.09	95.31	97.94	90.90	81.97	83.09
07.2021	94.26	29.11	86.62	95.40	96.44	73.10	92.48	0.00	0.00	0.00	94.03	94.09	89.14	96.62	90.29	89.02	93.66	86.27	94.56	91.68	91.80	94.45	89.58	78.23	72.67
06.2021	99.64	33.67	93.25	99.86	99.86	93.49	96.11	0.00	0.00	0.00	97.18	97.68	93.32	99.32	93.80	96.14	98.38	93.62	99.15	94.53	93.87	95.66	94.75	84.04	82.89
05.2021	99.74	45.98	89.98	99.63	99.84	82.47	84.25	0.00	0.00	84.74	92.58	98.04	90.93	98.57	82.29	91.06	98.45	74.57	99.38	68.63	68.48	97.15	89.44	85.03	83.69
04.2021	99.42	77.94	84.85	99.18	99.48	94.37	96.56	0.00	0.00	89.28	98.77	98.84	89.31	99.27	94.74	96.70	98.02	1.64	98.99	95.17	95.23	93.72	91.46	84.52	82.67
03.2021	99.60	59.43	88.59	96.23	75.91	91.36	92.75	0.00	0.00	25.13	98.92	98.90	87.55	99.74	91.81	92.57	98.09	1.64	99.12	89.61	89.69	93.51	91.27	73.92	80.21
02.2021	90.50	63.42	61.03	82.58	99.83	88.49	91.03	0.00	0.44	14.47	99.40	99.49	93.37	98.70	88.61	90.00	97.69	1.64	99.34	87.29	87.29	85.24	88.06	82.59	85.65
01.2021	99.96	64.61	81.95	85.11	99.82	95.10	97.44	0.00	41.66	26.32	99.53	99.61	88.28	99.98	95.35	95.72	97.49	1.64	81.75	92.36	92.50	90.49	93.94	66.85	74.55
12.2020	96.82	90.94	83.14	94.68	99.82	78.30	83.08	0.00	2.24	83.66	99.50	99.71	97.61	99.98	80.40	82.91	97.74	45.89	98.29	79.88	79.95	91.82	80.05	79.55	84.04
11.2020	99.68	69.82	91.27	99.70	99.59	77.62	84.28	0.00	82.59	95.89	99.32	99.40	97.23	99.78	81.94	83.09	98.49	82.67	99.11	81.26	81.31	89.94	82.50	80.86	83.37
10.2020	99.36	49.57	82.19	97.03	80.66	88.34	94.33	0.00	81.25	96.57	99.79	99.86	95.94	97.49	93.95	96.00	96.86	95.43	99.13	76.31	76.28	87.11	95.08	76.71	84.01
09.2020	98.96	61.18	86.12	96.43	7.90	82.29	81.85	0.00	69.53	96.01	15.76	99.91	94.91	99.99	83.53	82.42	98.22	78.12	92.52	82.18	82.21	87.77	38.27	78.73	81.43
08.2020	98.08	64.48	89.95	97.72	85.14	65.07	72.35	14.03	75.92	83.01	40.88	98.15	89.02	98.31	72.57	72.93	98.07	71.86	97.55	69.05	69.13	78.06	57.00	66.34	80.82
07.2020	99.51	82.65	85.23	99.07	49.67	72.86	75.18	62.58	15.53	82.32	99.91	99.96	91.43	99.26	75.78	76.63	99.89	75.44	98.74	72.99	73.00	89.83	75.28	68.29	84.08
06.2020	98.46	72.13	93.67	99.90	44.53	62.96	69.28	0.29	1.00	88.05	95.45	95.45	96.77	100.00	59.55	51.63	96.40	56.07	99.10	67.52	67.54	93.69	58.12	72.76	85.24
05.2020	97.76	35.14	98.24	98.58	30.96	24.90	55.70	21.37	30.02	98.33	100.00	99.93	91.23	100.00	55.37	1.64	98.28	1.64	80.28	52.73	52.75	35.73	38.14	53.99	71.47
04.2020	99.94	53.33	6.49	99.76	0.00	31.55	65.56	82.89	80.16	94.70	100.00	100.00	94.11	100.00	36.86	1.64	98.15	1.64	66.91	64.93	64.91	93.27	65.11	67.06	81.34
03.2020	99.80	22.40	29.08	99.64	0.00	33.95	56.94	85.20	80.67	98.23	100.00	100.00	95.46	100.00	1.64	38.55	98.25	34.35	99.54	56.02	56.08	90.91	56.39	66.41	82.73
02.2020	97.15	69.03	99.70	99.72	32.38	44.41	72.67	83.58	66.40	94.87	100.00	96.61	84.36	99.65	13.63	31.12	98.35	48.57	99.54	56.95	57.00	84.56	70.15	73.60	83.19
01.2020	99.93	25.27	99.61	98.93	34.30	49.97	75.14	64.48	0.00	72.04	98.97	98.97	85.59	99.99	45.82	71.73	64.48	73.72	98.33	73.78	73.86	54.17	74.19	67.25	69.43

Table 7. Real-time index values for the NM stations not used in the GLE Alert++. The colour coding is described in the text.

MM.YYYY	NMs Not Used in the Current Version of GLE Alert++ (from Table 2)														
	AATA	BRBG	CALG	DJON	DOMB	DOMC	DRBS	HRMS	JBGO	MWSN	MXCO	NANM	NRLK	PTFM	TSMB
08.2022	93.33	0.00	65.41	0.00	1.64	1.64	98.84	0.00	0.00	27.96	36.48	0.00	32.32	0.00	0.00
07.2022	6.01	1.64	0.00	0.00	1.64	1.64	99.44	0.00	0.00	26.20	36.23	0.00	42.65	0.00	0.00
06.2022	7.21	1.64	0.00	0.00	1.64	1.64	99.78	0.00	0.00	22.40	36.47	0.00	35.68	0.00	0.00
05.2022	0.00	1.64	0.00	0.00	1.64	1.64	99.93	0.00	0.00	17.17	36.46	0.00	84.17	0.00	0.00
04.2022	0.00	1.64	0.00	0.00	1.64	1.64	99.84	0.00	0.00	23.66	36.48	0.00	84.54	0.00	0.00
03.2022	0.00	1.63	0.00	0.00	1.64	1.64	96.26	0.00	0.00	22.02	36.46	0.00	75.74	0.00	0.00
02.2022	0.00	1.64	0.00	0.00	1.64	1.64	88.91	0.00	0.00	22.58	36.42	0.00	77.60	0.00	0.00
01.2022	0.00	1.64	0.00	0.00	1.64	1.64	97.12	0.00	0.00	22.61	36.43	0.00	73.80	0.00	0.00
12.2021	0.00	1.64	0.00	0.81	1.64	1.52	98.78	0.00	0.66	22.22	36.45	0.00	74.16	0.00	0.00
11.2021	16.87	1.64	0.00	0.77	1.64	1.38	96.41	0.00	0.71	20.18	35.89	0.00	83.38	0.00	0.00
10.2021	0.09	1.62	0.00	0.90	1.64	1.64	99.95	0.00	0.73	13.39	36.42	0.00	71.45	0.00	0.00
09.2021	31.86	1.63	0.00	0.71	1.64	1.64	96.71	0.00	0.68	16.89	36.46	0.00	59.17	0.00	0.00
08.2021	79.18	1.64	0.00	0.69	1.64	1.64	98.77	0.00	0.29	22.72	33.63	0.00	65.70	0.00	0.00
07.2021	51.61	1.64	0.00	0.74	1.64	1.64	96.31	0.00	0.75	21.89	34.73	0.00	76.70	0.00	0.00
06.2021	60.76	1.64	0.00	0.00	1.64	1.64	82.24	0.00	0.76	23.67	36.33	0.00	82.40	0.08	0.00
05.2021	86.30	1.64	0.00	0.00	1.64	1.64	99.88	0.00	0.83	19.13	36.38	58.92	80.80	0.81	0.00
04.2021	92.26	1.64	0.00	1.07	1.64	1.64	98.68	0.00	0.75	24.21	36.05	92.58	80.13	1.05	0.00
03.2021	70.81	1.64	0.00	0.73	1.64	1.64	97.83	0.00	0.80	19.21	35.90	80.72	77.68	1.64	0.00
02.2021	87.67	1.64	0.00	0.73	1.64	1.64	96.85	0.04	0.86	23.84	31.87	93.20	14.51	1.64	0.00
01.2021	87.10	1.64	0.00	0.76	1.64	1.64	98.34	0.00	0.83	17.78	1.74	80.68	43.23	1.64	0.00
12.2020	58.52	1.64	0.00	0.00	1.64	1.64	93.04	0.00	0.78	20.31	1.74	57.47	26.04	1.48	0.00
11.2020	66.68	1.62	0.00	0.00	0.05	1.64	99.72	0.00	0.75	9.76	1.76	43.22	84.27	1.29	0.00
10.2020	50.41	1.63	0.00	0.00	0.00	1.64	93.59	0.00	0.78	23.67	1.75	94.02	49.93	1.54	0.00
09.2020	83.23	1.64	0.00	0.00	0.00	1.64	1.62	0.00	0.78	23.21	1.72	93.88	70.35	1.58	0.00
08.2020	90.11	1.63	0.00	0.00	0.00	1.64	1.64	0.00	0.79	23.20	1.41	91.65	66.96	1.47	0.00
07.2020	82.11	1.62	0.00	0.00	0.00	1.56	1.64	1.28	39.92	24.85	1.59	94.23	73.52	1.58	0.27
06.2020	93.58	1.64	0.00	0.00	0.00	1.52	37.34	1.56	32.64	22.20	1.74	91.84	71.39	2.13	0.32
05.2020	90.51	1.63	0.00	0.00	0.00	1.64	77.84	1.64	0.78	22.75	1.74	86.54	85.75	1.50	0.38
04.2020	96.30	1.64	0.00	0.00	0.00	1.54	1.62	1.64	0.73	8.02	1.74	91.95	87.22	1.24	0.53
03.2020	59.22	1.64	0.00	0.00	0.00	1.64	1.64	67.89	0.81	1.43	1.74	88.34	86.05	82.27	62.66
02.2020	72.95	1.64	0.00	0.16	0.00	1.64	65.27	67.20	1.29	1.51	1.74	93.48	83.23	64.09	55.57
01.2020	99.73	1.64	0.00	0.77	0.00	1.64	3.10	73.54	1.54	1.34	1.74	68.27	36.96	64.78	43.58

4. Discussion and Conclusions

The assessment of the GLE Alert ++ was concluded in October 2022 and focused on: (a) the availability of the real-time data provided by the NM stations that contribute to the GLE Alert++, (b) the behaviour of each station regarding the different levels of alert (watch, warning and alert), and (c) the definition of the real-time assessment index (the real-time behaviour is not only correlated with the measurement delays, but also with the existence of all measurements (i.e., the integral of the frequency)). In order to identify if the station should be used by the GLE Alert++ service, the availability of the real-time data and the data flow of each station was examined. No conclusions were drawn about the quality of the cosmic ray data, as this is the responsibility of the principal investigator of each NM station. The aim of this work is to evaluate the reliability of the GLE alert system that is based on, and derived from, a scientific scenario of cosmic ray physics. In order to achieve this, it was essential to delve into technical considerations.

The main results of this study are summarized as follows:

1. The GLE Alert++ service needs timely and reliable real-time data
2. GLE Alert++ uses historical NM data to validate and optimize the algorithm (access to the data, whether real-time or not, of all NM stations is therefore crucial for this study)
3. A total of eight stations (BURE, ESOI, MCMU, MCRL, MGDN, MOSC, MRNY, NVBK) are constantly offline.
4. Station LMKS cannot be evaluated because all required information was not available in the NMDB.
5. The ATHN station was delayed until 02/2022 because of a problem with the clock of the NM registration system. The measurements were however instantly sent to NMDB with a delay timestamp, due to the clock's delay. This problem has now been fixed.
6. The DRBS NM station (currently not used by the GLE Alert++ and listed in Table 2) presents an acceptable real-time behaviour.

On the basis of this assessment study, the Station Table used by the GLE Alert++ service has been updated, and now includes 27 NM stations, including 26 of the original 34 (BURE, ESOI, MCMU, MCRL, MGDN, MOSC, MRNY, NVBK are excluded), and a new one (DRBS).

With regard to these stations, it has been concluded that the great majority of stations follow the distribution of watch, warning and alert states. However, a few stations enter alert state more often than expected, which statistically increases the probability of false alert. This conclusion does not lead to these stations being excluded, but does affect the trustfulness of the interval that should be used in these cases.

According to the real-time assessment index values, in some months stations exceed the optimal case of the 15 min equivalent delay, which is 77.05. This does not affect the operation of the service but only the moment when the alert is raised. Even the delayed data are useful for the GLE Alert++ service.

Finally, it is suggested that the assessment of the real-time availability of the NM data must be repeated periodically (every 2 years), in order to update the set of the NM stations used in GLE Alert++, as the operating conditions of some stations frequently change. It should be noted that the radiation exposure of aviation flights to cosmic rays has become a contemporary subject of great concern to the scientific community over the last few years [20–23]. The results of this study highlight that the NM database that feeds the GLE Alert++ system is trustworthy, enabling it to function as a reliable and trustworthy warning tool. In turn, this tool could not only be used to calculate radiation exposure but also to protect human health during space weather phenomena. This study reveals that the optimal running of the system can be ensured by periodically assessing and updating the set of NM stations used in GLE Alert++.

Author Contributions: Software, P.P. and A.S.; data curation, M.G. and M.L.; writing—original draft preparation, D.L., M.-C.P. and A.T.; writing—review and editing, N.C. and M.D.; supervision, H.M. All authors have read and agreed to the published version of the manuscript.

Funding: This work is supported by ESA SSA SWE Space Radiation Expert Service Centre activities (ESA contract number 4000113187/15/D/MRP) and the ESA Space Safety Programme's network of space weather service development and pre-operational activities (ESA contract number 4000134036/21/D/MRP). The European Neutron Monitor Services research is funded by ESA SSA SN IV-3 Tender: RFQ/3-13556/12/D/MRP. The high-resolution Neutron Monitor Database (NMDB), is funded by the European Union. A.Ne.Mo.S is supported by the Special Research Account of Athens University (70/4/5803).

Institutional Review Board Statement: Not applicable.

Informed Consent Statement: Not applicable.

Data Availability Statement: Data of neutron monitors available at www.nmdb.eu.

Acknowledgments: The authors would like to thank the cosmic ray data providers of the high-resolution Neutron Monitor Database (NMDB).

Conflicts of Interest: The authors declare no conflicts of interest.

References

- Miroshnichenko, L.I. Retrospective analysis of GLEs and estimates of radiation risks. *J. Space Weather Space Clim.* **2018**, *8*, A52. [[CrossRef](#)]
- Poluianov, S.V.; Usoskin, I.G.; Mishev, A.L.; Shea, M.A.; Smart, D.F. GLE and Sub-GLE Redefinition in the Light of High-Altitude Polar Neutron Monitors. *Solar Phys.* **2017**, *292*, 176. [[CrossRef](#)]
- Mishev, A.L.; Kocharov, L.G.; Usoskin, I.G. Analysis of the ground level enhancement on 17 May 2012 using data from the global neutron monitor network. *J. Geophys. Res. Space Phys.* **2014**, *119*, 670–679. [[CrossRef](#)]
- Bütikofer, R.R.; Flückiger, E.O.; Desorgher, L.; Moser, M.; Pirard, B. The solar cosmic ray ground-level enhancements on 20 January 2005 and 13 December 2006. *Adv. Space Res.* **2009**, *43*, 499–503. [[CrossRef](#)]
- Papaioannou, A.; Kouloumvakos, A.; Mishev, A.; Vainio, R.; Usoskin, I.G.; Herbst, K.; Rouillard, A.P.; Anastasiadis, A.; Gieseler, J.; Wimmer-Schweingruber, R.F.; et al. The first ground-level enhancement of solar cycle 25 on 28 October 2021. *Astron. Astrophys.* **2022**, *660*, 9. [[CrossRef](#)]
- Malandraki, O.E.; Crosby, N.B. Solar energetic particles and space weather: Science and applications. In *Solar Particle Radiation Storms Forecasting and Analysis*; Malandraki, O.E., Crosby, N.B., Eds.; Springer International Publishing: Berlin/Heidelberg, Germany, 2018; Volume 444, pp. 1–26.
- Maurchev, E.A.; Shlyk, N.S.; Dmitriev, A.V.; Abunina, M.A.; Didenko, K.A.; Abunin, A.A.; Belov, A.V. Comparison of Atmospheric Ionization for Solar Proton Events of the Last Three Solar Cycles. *Atmosphere* **2024**, *15*, 151. [[CrossRef](#)]
- Poluianov, S.; Batalla, O.; Mishev, A.; Koldobskiy, S.; Usoskin, I. Two New Sub-GLEs Found in Data of Neutron Monitors at South Pole and Vostok: On 09 June 1968 and 27 February 1969. *Sol. Phys.* **2024**, *299*, 6. [[CrossRef](#)]
- Gopalswamy, N.; Yashiro, S.; Liu, Y.; Michalek, G.; Vourlidas, A.; Kaiser, M.L.; Howard, R.A. Coronal mass ejections and other extreme characteristics of the 2003 October–November solar eruptions. *J. Geophys. Res.* **2005**, *110*, A09S15. [[CrossRef](#)]
- Gopalswamy, N. A Catalog of Halo Coronal Mass Ejections from SOHO. *Sun Geosph.* **2010**, *5*, 7–16.
- Gopalswamy, N.; Xie, H.; Yashiro, S.; Akiyama, S.; Mäkelä, P.; Usoskin, I.G. Properties of Ground Level Enhancement Events and the Associated Solar Eruptions During Solar Cycle 23. *Space Sci. Rev.* **2012**, *171*, 23–60. [[CrossRef](#)]
- Shea, M.A.; Smart, D.F. A summary of major solar proton events. *Sol. Phys.* **1990**, *127*, 297–320. [[CrossRef](#)]
- Shea, M.A.; Smart, D.F. Significant Solar Proton Events for Five Solar Cycles (1954–2007). In Proceedings of the 30th ICRC, Merida, Mexico, 3–11 July 2007.
- Kuwabara, T.; Bieber, J.W.; Clem, J.; Evenson, P.; Pyle, R.; Munakata, K.; Yasue, S.; Kato, C.; Akahane, S.; Koyama, M.; et al. Real-time cosmic ray monitoring system for space weather. *Space Weather* **2006**, *4*, S08001. [[CrossRef](#)]
- Anashin, V.; Belov, A.V.; Eroshenko, E.; Kryakunova, O.; Mavromichalaki, H.; Ishutin, I.; Sarlanis, C.; Souvatzoglou, G.; Vashenyuk, E.; Yanke, V. The ALERT signal of ground level enhancements of solar cosmic rays: Physics basis, the ways of realization and development. In Proceedings of the 31st ICRC, Łódź, Poland, 7–15 July 2009.
- Mavromichalaki, H.; Souvatzoglou, G.; Sarlanis, C.; Mariatos, G.; Papaioannou, A.; Belov, A.; Eroshenko, E.; Yanke, V.; NMDB team. Implementation of the ground level enhancement alert software at NMDB database. *New Astron.* **2010**, *15*, 744–748. [[CrossRef](#)]
- Souvatzoglou, G.; Papaioannou, A.; Mavromichalaki, H.; Dimitroulakos, J.; Sarlanis, C. Optimizing the real-time ground level enhancement alert system based on neutron monitor measurements: Introducing GLE Alert Plus. *Space Weather* **2014**, *12*, 633–649. [[CrossRef](#)]
- Mavromichalaki, H.; Paschalis, P.; Gerontidou, M.; Papailiou, M.-C.; Paouris, E.; Tezari, A.; Lingri, D.; Livada, M.; Stassinakis, A.N.; Crosby, N.; et al. The Updated Version of the A.Ne.Mo.S. GLE Alert System: The Case of the Ground-Level Enhancement GLE73 on 28 October 2021. *Universe* **2022**, *8*, 378. [[CrossRef](#)]

19. Sapundjiev, D.; Verhulst, T.; Stankov, S. International Database of Neutron Monitor Measurements: Development and Applications. In *Knowledge Discovery in Big Data from Astronomy and Earth Observation*; Škoda, P., Adam, F., Eds.; Elsevier: Amsterdam, The Netherlands, 2020.
20. Malandraki, O.E.; Nunez, M.; Heber, B.; Labrenz, J.; Posner, A.; Milas, N.; Tsiropoula, G.; Pavlos, E.; Sarlanis, C. The real-time SEP forecasting tools of the 'HESPERIA' HORIZON 2020 project. EGU General Assembly Conference Abstracts. 2017. Available online: <https://ui.adsabs.harvard.edu/abs/2017EGUGA..1919268M/abstract> (accessed on 8 March 2024).
21. Núñez, M.; Reyes-Santiago, P.J.; Malandraki, O. Real-time prediction of the occurrence of GLE events. *Space Weather* **2017**, *15*, 861–873. [[CrossRef](#)]
22. Flückiger, E.; Bütikofer, R. Radiation doses along selected flight profiles during two extreme solar cosmic ray events. *ASTRA* **2011**, *7*, 105–109.
23. Mishev, A.L.; Usoskin, I.G. Assessment of the radiation environment at commercial jet-flight altitudes during GLE 72 on 10 September 2017 using neutron monitor data. *Space Weather* **2018**, *16*, 1921–1929. [[CrossRef](#)]

Disclaimer/Publisher's Note: The statements, opinions and data contained in all publications are solely those of the individual author(s) and contributor(s) and not of MDPI and/or the editor(s). MDPI and/or the editor(s) disclaim responsibility for any injury to people or property resulting from any ideas, methods, instructions or products referred to in the content.